Modeling *ZNF408*-Associated FEVR in Zebrafish Results in Abnormal Retinal Vasculature

Dyah W. Karjosukarso,[1] Zaheer Ali,[2] Theo A. Peters,[3] Jia Qi Cheng Zhang,[1] Anita D.M. Hoogendoorn,[1] Alejandro Garanto,[1] Erwin van Wijk,[3] Lasse D. Jensen,[2] and Rob W.J. Collin[1]

[1]Department of Human Genetics, Donders Institute for Brain, Cognition and Behaviour, Radboud University Medical Center, Nijmegen, The Netherlands
[2]Unit of Cardiovascular Medicine, Department of Medical and Health Sciences, Linköping University, Linköping, Östergötland, Sweden
[3]Department of Otorhinolaryngology, Donders Institute for Brain, Cognition and Behaviour, Radboud University Medical Center, Nijmegen, The Netherlands

Correspondence: Rob W.J. Collin, Geert Grooteplein 10, 6525 GA Nijmegen, The Netherlands; rob.collin@radboudumc.nl.
Lasse D. Jensen, Linköping University, Campus US, Entrance 68, Pl. 08, SE-58183 Linköping, Sweden; lasse.jensen@liu.se.

LDJ and RWJC contributed equally to this work and are both corresponding authors.

Purpose. Familial exudative vitreoretinopathy (FEVR) is an inherited retinal disease in which the retinal vasculature is affected. Patients with FEVR typically lack or have abnormal vasculature in the peripheral retina, the outcome of which can range from mild visual impairment to complete blindness. A missense mutation (p.His455Tyr) in *ZNF408* was identified in an autosomal dominant FEVR family. Little, however, is known about the molecular role of ZNF408 and how its defect leads to the clinical features of FEVR.

Methods. Using CRISPR/Cas9 technology, two homozygous mutant zebrafish models with truncated *znf408* were generated, as well as one heterozygous and one homozygous missense *znf408* model in which the human p.His455Tyr mutation is mimicked.

Results. Intriguingly, all three *znf408*-mutant zebrafish strains demonstrated progressive retinal vascular pathology, initially characterized by a deficient hyaloid vessel development at 5 days postfertilization (dpf) leading to vascular insufficiency in the retina. The generation of stable mutant lines allowed long-term follow up studies, which showed ectopic retinal vascular hyper-sprouting at 90 dpf and extensive vascular leakage at 180 dpf.

Conclusions. Together, our data demonstrate an important role for *znf408* in the development and maintenance of the vascular system within the retina.

Keywords: CRISPR/Cas9, FEVR, retinal vasculature, zebrafish, znf408

Vasculature defects in the retina are one of the leading causes of visual impairment.[1] Different developmental vision disorders resulting from retinal vasculature defects have been described, such as familial exudative vitreoretinopathy (FEVR), Norrie disease, persistent fetal vasculature, and retinopathy of prematurity (ROP), some of which have overlapping features.[2] FEVR is a rare inherited disorder hallmarked by an abnormal development of the vasculature in the peripheral retina. The clinical features of FEVR are heterogeneous, varying from normal vision to complete blindness.[2] Besides its diverse clinical manifestations, FEVR is also a genetically heterogeneous disorder. Defects in *FZD4*, *LRP5*, *NDP*, and *TSPAN12* are classically associated with FEVR. These genes, as well as the mutations they harbor, have been thoroughly investigated *in vitro* and *in vivo* (reviewed by Gilmore and Nikopoulos et al.).[2,3] Recent genetic studies discovered more genes to be associated with FEVR, such as *ZNF408*,[4] *RCBTB1*,[5] and *CTNNB1*.[6,7]

A missense mutation in *ZNF408* (c.1363C>T, p.His455Tyr, NM_024741) was identified in a large autosomal dominant FEVR family.[4] We demonstrated that the encoded protein, ZNF408, is localized in the nucleus and the mutation caused mislocalization of ZNF408 to the cytoplasm.[4] Furthermore, morpholino-induced transient knockdown of *znf408* in zebrafish led to abnormal development of eye and trunk vasculature,[4] suggesting it plays an important role in the development of the vasculature. However, it remains unclear what the exact role of ZNF408 is in this process, as well as how its defect results in abnormal retinal vasculature development that leads to visual impairment.

In the recent years, zebrafish has become more and more popular as a model organism to study disease mechanisms. Besides their easy maintenance and relatively low cost, 84% of known human disease-associated genes have an ortholog in this model.[8] Vision-related disorders are among the wide variety of human diseases that have been studied in zebrafish. The zebrafish retina has a layered structure that is highly similar to the human retina. Because zebrafish are diurnal organisms, their cone density is also close to that of the human retina.[9] Furthermore, the zebrafish retina is

supplied by a choroidal and a retinal vasculature, the latter being derived from the hyaloid vasculature, comparable to the retinal vasculature in humans.[10–12] Finally, the availability of transgenic zebrafish lines expressing fluorescent reporters in the cells that constitute the blood vessels, such as *Tg(fli1:GFP)*[13] and *Tg(flk1:GFP)*,[14] adds an extra advantage in its application to studies of vascular-related disorders.

Although a previous morpholino-mediated knockdown study has shown that znf408 is crucial in the development of eye and trunk vasculature in zebrafish,[4] the specificity of morpholinos has been debated over the recent years.[15–17] Moreover, transient knock-down merely allows short-term investigation during early development. Finally, only the effect of an insufficient amount of a protein of interest could be observed in such knock-down studies, which is not always completely relevant for diseases inherited in an autosomal dominant manner, such as FEVR. To further study the role of ZNF408 in the vasculature development *in vivo*, we generated two homozygous zebrafish models with a frameshift mutation in *znf408* (*znf408^{rmc103/rmc103}* and *znf408^{rmc104/rmc104}*), as well as one heterozygous and one homozygous missense *znf408* model in which the human p.His455Tyr mutation is mimicked (*znf408^{rmc105/+}* and *znf408^{rmc105/rmc105}*), using CRISPR/Cas9 technology. This study was designed to determine the effect of absence (or truncation) of znf408 as well as the effect of a specific amino acid substitution as observed in FEVR patients, which may or may not differ from the effect of *znf408* knockdown. Furthermore, the generation of stable mutant zebrafish lines allowed us to study and compare the effect of the mutations from larval stage up to adult stage, whereas the previous knockdown study only allowed observation at larval stage. We found that both the absence of znf408 as well as the presence of znf408 harboring the human FEVR-mutation resulted in impaired development of the hyaloid vasculature, followed by subsequent hyper-sprouting and structural destabilization of retinal vessels in the periphery of the optic disc culminating in extensive retinal vascular leakage at 180 days postfertilization (dpf). These phenotypes accurately recapitulate the disease history of FEVR in human patients, suggesting that the zebrafish mutants developed here could be exploited for developing an improved understanding of FEVR.

Materials and Methods

Ethics Statement

Zebrafish experiments were approved by the local Animal Experimentation Committee (RU-DEC-2016-0991 and N89/15) and were performed according to the Dutch law (Wet op Dierproven 1996), the Swedish guidelines for laboratory animal research, and European regulations (Directive 86/609/EEC). The study was performed in adherence to the ARVO Statement for the Use of Animals in Ophthalmic and Vision Research.

Zebrafish Husbandry

Tupfel long fin and *Tg(flk1:GFP)* zebrafish were maintained under standard conditions following institutional and international guidelines. Zebrafish eggs were obtained from natural spawning.

CRISPR/Cas9 Design

The zebrafish znf408 protein sequence was aligned with the human ZNF408 protein using AlignX in VectorNTI software package to determine the position of the fourth zinc finger domain in zebrafish znf408 (Figure S1). Subsequently, guide RNAs (gRNAs) targeting the nucleotide sequences around the fourth zinc finger domain (Fig. 1a) were designed using Chopchop software (https://chopchop.rc.fas.harvard.edu/) and synthesized as previously described by Gagnon et al.[18] A single-stranded DNA donor template was used to generate the mutation that changes one of the histidine residues in the fourth zinc finger domain to a tyrosine, similar to the human p.His455Tyr mutation (Fig. 1a). Next to the intended mutation, the donor template also contained silent mutations to avoid recognition by the gRNA (Fig. 1a).

Generation of ZNF408 Zebrafish Model

To increase the efficiency of the homology directed repair mechanism, the nonhomologous end joining repair mechanism was inhibited by a splice-blocking morpholino targeting *ku70* (5′-AACTTTTTAGGCTCACCTGCATAGT-3′).[19,20] A mix of 1 nL containing donor template (0.3 μM), gRNA (600 pg), Cas9 protein (5 ng), *ku70* morpholino (1.5 ng), phenol-red (0.01%), and KCl 0.2 M was injected using a Pneumatic Picopump pv280 (World Precision Instruments) into zebrafish embryos at a one-cell stage. The injected embryos were grown into adulthood at 28°C in E3 medium (5 mM NaCl, 0.17 mM KCl, 0.33 mM CaCl$_2$, 0.33 mM MgSO$_4$, supplemented with 0.01% methylene blue). Three months postfertilization, adult CRISPR-injected fish were in-crossed. The offspring was raised and individually genotyped. Subsequently, the appropriate *znf408* mutants were crossed with *Tg(flk1:GFP)* fish to generate zebrafish with modified *znf408* and a GFP reporter on the blood vessels (Fig. 1b). The generated fish were then in-crossed to generate homozygous models (Fig. 1b).

Genotyping

Larvae and adult fish were genotyped by lysing the larvae or the fin of the adult fish in lysis buffer (40 mM NaOH and 0.2 mM EDTA) for 20 minutes at 95°C. For PCR amplification targeting the mutated region, 1 to 4 μL of the 10 times diluted lysate was used. The primers fw 5′-GTGCACAGAGTGTGGCAAGT-3′ and rev 5′-CACGTTGGCGAAAACACTTA-3′ were used for *znf408* genotyping and subsequent Sanger sequencing.

RNA Analysis

For each RNA isolation, a pool of 25 zebrafish larvae was used. The larvae were snap frozen in liquid nitrogen at 2 dpf and either stored at -80°C or directly used for RNA isolation. The larvae were homogenized in Qiazol (Qiagen, Hilden, North Rhein Westphalia, Germany). The homogenized larvae were subjected to overnight chloroform:isopropanol precipitation using glycogen as a carrier. The precipitated RNA was subsequently purified using the Nucleospin RNA kit (Macherey Nagel, Düren, North Rhein Westphalia, Germany) following the manufacturer's instructions. cDNA was synthesized from 500 to 1000 ng RNA using the iScript cDNA (Bio-rad, Hercules, CA, United States) synthesis kit. The obtained cDNA was used as template for *znf408*
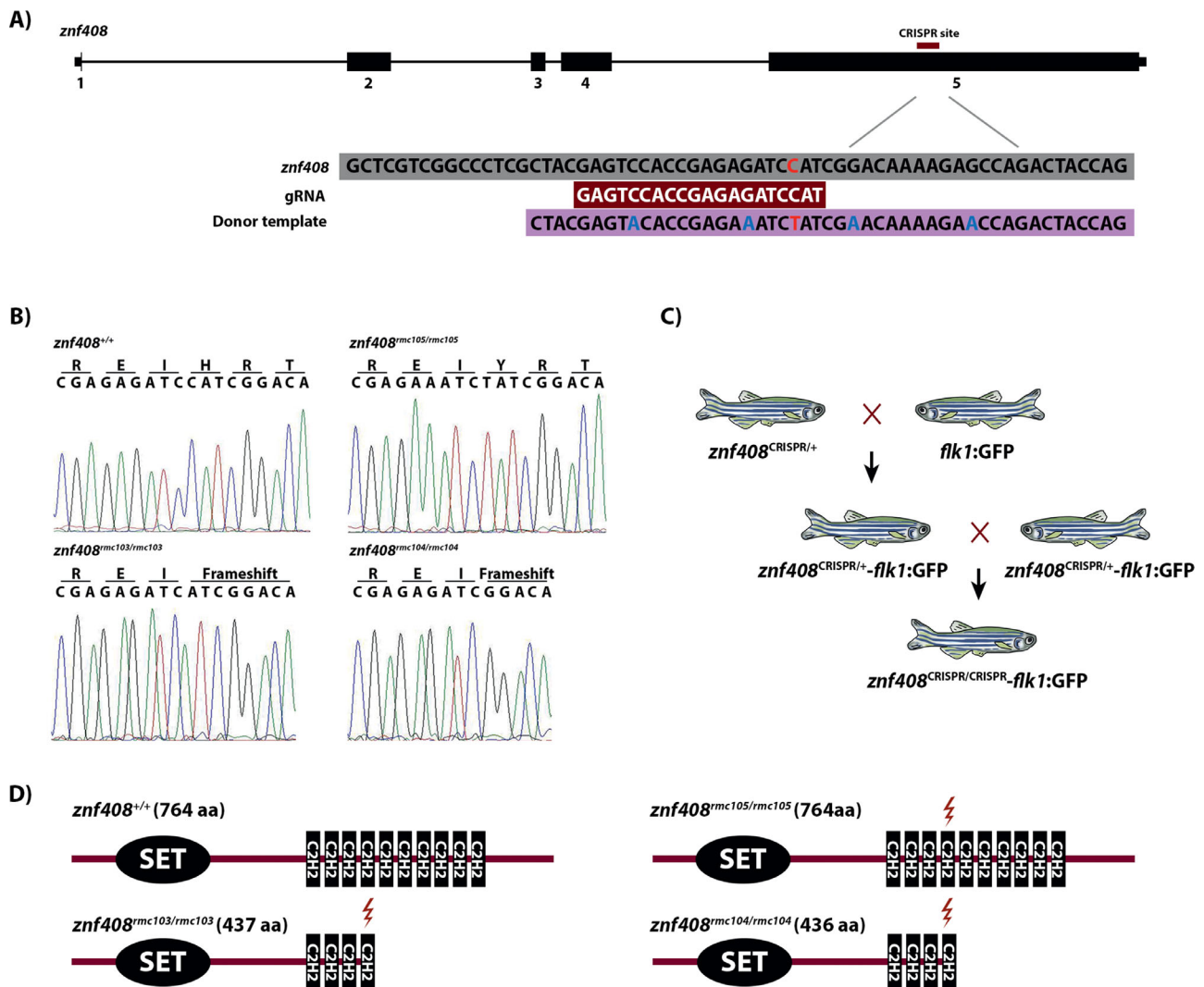
FIGURE 1. Generation of *znf408* zebrafish models. (**a**) The 5 exons of zebrafish *znf408* are shown. The sequences targeted in exon 5 as well as gRNA and donor template sequences are indicated. (**b**) Sequence analysis of wild type *znf408*, *znf408*[c.1282C>T], *znf408*[c.1282del], and *znf408*[c.1282_1285del]. (**c**) The crossing of *znf408* mutants with *Tg(flk1:GFP)* line. (**d**) Protein prediction of the *znf408* mutants generated by Prosite tool (https://prosite.expasy.org/scanprosite/) based on the amino acid sequences. The length of the predicted mutant proteins is indicated.

amplification using the same primers as used for genotyping. The product of this amplification was also Sanger sequenced to ensure that the mutation is transcribed into the mRNA. For quantitative PCR (qPCR), the following primers were used: fw 5′-CAACACTTCAGATCACTTCTCAGG-3′ and rev 5′-CATTCTGCTCAAGGACATTGG-3′. For normalization purposes, *actb*1 was amplified using primers fw 5′-CAACAGGGAAAAGATGACACAGAT-3′ and rev 5′-CAGCCTGGATGGCAACGT-3′. qPCR analysis was performed in duplicate.

Immunohistochemistry

Zebrafish larvae at 5 dpf were incubated for 10 minutes in 10% (w/v) sucrose/PBS solution for cryoprotection, followed by embedding in optimal cutting temperature reagent and snap freezing in isopentane cooled in a liquid nitrogen bath. The cryosections (7 μm) were fixed in 4% paraformaldehyde for 10 minutes at room temperature followed by permeabilization in 0.01% (v/v) Tween 20/PBS for 20 minutes at room temperature. Subsequently, the cryosections were blocked in 10% normal goat serum and 2% BSA for 1 hour at room temperature. The immunostaining was performed overnight using the following primary antibodies: rabbit anti-znf408 antibody (1:100, Sigma, St. Louis, MO, United States) and rabbit anti-GNAT2 (1:500, MBL, Woburn, MA, United States). The sections were washed 3 times 5 minutes with PBS and then subjected to secondary antibody and DAPI incubation for 1 hour at room temperature. The secondary antibodies used were goat-anti-rabbit Alexa Fluor 568 (1:800, Molecular Probes, Thermo Fisher Scientific, Waltham, MA, United States). For Bodipy staining, cryosections were permeabilized with 0.5% Triton X-100 followed by 20 minutes incubation in Bodipy (1:5000, Life Technologies, Carlsbad, CA, United States) and DAPI. Subsequent to washing with PBS, sections were mounted using ProLong Gold (Thermo

Fisher Scientific). Images were taken with Zeiss Axio Imager Z2 (Zeiss, Oberkochen, Baden-Württemberg, Germany). The obtained images were analyzed using ZEN3.0 software. At least three sections were analyzed for outer segment (OS) length, outer nuclear layer thickness, and inner nuclear layer thickness. Differences between the groups were evaluated using ANOVA followed by Dunnett's post hoc test, $P < 0.05$ was considered statistically significant.

Vascular Phenotyping

Vascular density, morphology, and leakage were evaluated by confocal microscopy in the retina of zebrafish larvae at 5 dpf, young adults at 90 dpf, or adults at 180 dpf, following intravenous or intraperitoneal injection in larvae or adults, respectively, of lysine-modified, rhodamine-conjugated dextran at 70 kDa (Thermo Scientific), 30 minutes before euthanasia with 0.04% MS-222. Euthanized fish were then fixed overnight at 4°C in 4% paraformaldehyde, enucleation was performed and, in the case of the adult eyes, the cornea, lens, and sclera was removed as previously described.[21,22] Tissues were mounted, vitreal side up in VectaShield (Vector, Burlingame, CA, United States) and visualized using an LSM700 upright confocal microscope (Leica, Wetzlar, Hesse, Germany). Numbers of completed and anastomosed vessels or incomplete sprouts were manually counted from confocal images of hyaloid/retinal vascular areas of a specified size and density was measured as the percentage of green pixels (i.e., endothelial area) in the total area. Numbers of completed hyaloid vessels, hyaloid or retinal sprouts and the vascular densities were analyzed in a total of 6 to 10 individual fish per group. The plasma content in the tissue was determined as the percentage of leaked dextran (i.e., red pixels in dual-color images) in an area of interest. Leakage was determined as the plasma content in the tissue divided by the total amount of dextran-containing plasma in the area (i.e., red plus yellow pixels, the latter representing nonleaked, luminal dextran characterized by overlapping green and red signals). Plasma tissue content and leakage was analyzed in a total of five to eight individual fish per group. Differences between the groups were evaluated using ANOVA followed by Dunnett's post hoc test and $P < 0.05$ was considered significant.

Visual Motor Response Assays

Visual motor response assays were performed on zebrafish larvae at 5 dpf using a Danio Vision Observation Chamber (Noldus, Wageningen, Gelderland, the Netherlands). The larvae were individually placed in each well of a 48-well plate and subjected to 20 minutes habituation in the dark, followed by cycles of 10 minutes lights OFF (dark) and 10 minutes lights ON (light) for 4 hours at 28°C. For every batch of larvae, the assay was performed once in the morning and once in the afternoon using different sets of larvae. At least three independent morning and afternoon assays were performed for each genotype. Distance moved (DM, in mm) and maximum velocity (Vmax, in mm/s) were tracked per larvae per second using EthoVision software (Noldus). Average DM and average Vmax of 24 wild-type larvae were compared with the average activity of 24 mutant larvae in each assay. Further, we focused our analysis on the startle response of the larvae to drastic light onset (change from lights OFF to lights ON). Delta DM and delta Vmax were calculated for each light onset in each assay. Delta DM or delta Vmax was defined as average DM or Vmax at light ON+1 second and light ON+2 seconds subtracted by the average DM or Vmax 30 seconds before lights ON. Delta DM and delta Vmax of each light onset from at least three morning or afternoon assays were averaged and compared between those of wild-type larvae and mutant larvae. A two-tailed unpaired Student *t*-test was used to calculate the significant difference between wild-type and mutant larvae at each light onset. The obtained *P* values were subjected to multiple testing corrections using the Benjamini-Hochberg method. All analyses were performed using R, version 3.3.1.

RESULTS

CRISPR/Cas9 technology was employed to generate mutant *znf408* zebrafish models. A gRNA was designed to specifically target *znf408* around the nucleotides coding for the fourth zinc finger domain (Fig. 1a). A single-stranded oligonucleotide containing the intended *znf408* c.1282C>T change was designed as donor template, flanked by 25 nucleotides long homology arms. A few silent mutations were inserted in the homology arms to avoid recognition by gRNA (Fig. 1a). A mixture of gRNA, donor template, and Cas9 protein was injected into one-cell staged zebrafish embryos (F0). Several genotypes were identified in adult F1 fish, including c.1282del (*znf408*[rmc103/+]), c.1282_1285del (*znf408*[rmc104/+]), and c.1282C>T (*znf408*[rmc105/+]) (Fig. 1b). F1 fish with these genotypes were individually crossed with *Tg(flk1:GFP)* fish to generate a zebrafish line with both modified *znf408* and GFP reported on the blood vessels. The generated heterozygous fish were crossed with each other to generate homozygous fish (Fig. 1c) such that both heterozygous mutant (mimicking FEVR) as well as homozygous mutant (mimicking retinitis pigmentosa) fish could be studied. RT-PCR analysis showed that in all *znf408* mutant larvae (2 dpf) the mutant mRNAs were expressed, indicating that the mutant transcripts do not fully undergo nonsense-mediated decay (Fig. 2a). Surprisingly, real-time qPCR analysis showed that *znf408* expression appeared to be a bit higher in, especially, the homozygous mutant zebrafish lines, compared with wild-type zebrafish (Fig. 2b).

The c.1282del and c.1282_1285del mutations lead to a frameshift and are predicted to generate shorter proteins that are truncated from the fourth zinc finger domain onwards, whereas c.1282C>T changes one of the core histidine residues in the fourth zinc finger domain to a tyrosine (p.His428Tyr), at the orthologous position of the p.His455Tyr mutation in human ZNF408 (Fig. 1d). In each mutant generated, the predicted fourth zinc finger domain is disrupted due to the mutations introduced. We attempted to determine (mutant) znf408 protein expression by using one of the antibodies directed against human ZNF408. As demonstrated in Supplemental Figure S1, the region of the epitope is not well conserved between human and zebrafish proteins, nor should it recognize the truncated protein potentially present in the *znf408*[rmc103/rmc103] and *znf408*[rmc104/rmc104] mutants. Immunohistochemistry of 5 dpf larvae, however, revealed "znf408" staining in the outer plexiform layer, both in the wild-type and in all mutant conditions (Supplemental Fig. S2), suggesting the observed staining is nonspecific. Znf408 was not clearly detectable in the eyes of 3 mpf fish by immunostaining (Supplemental Fig. S3) nor in the eyes of 6 mpf fish (data not shown), even though *znf408* transcripts were detectable in the eyes of 90 dpf and 180 dpf fish (Fig. 2c).
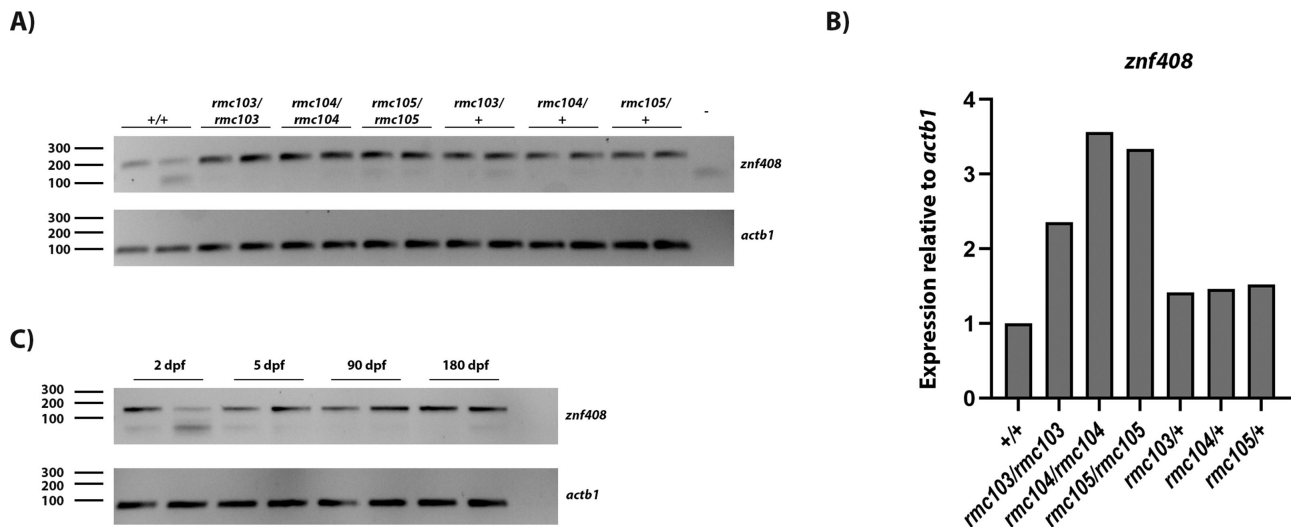
FIGURE 2. RT-PCR analysis of *znf408* transcripts. (**a**) *znf408* is expressed in wild-type and mutant larvae at 2 dpf. Two biological replicates are shown. (**b**) Quantitative measurement of *znf408* expression in wild-type and mutant larvae via qPCR analysis. *Znf408* expression is shown as a mean of two biological replicates shown in (**a**). (**c**) *znf408* is expressed at 2 dpf and 5 dpf larvae as well as in the eye of 3 mpf and 6 mpf wild-type fish. Two biological replicates are shown.

To determine the overall retinal integrity in the various mutant lines, retinal sections were stained for Bodipy, a marker for photoreceptor OS. As can be observed in Fig. 3a and b, overall OS length was not strikingly different between wild-type and *znf408* mutant lines, although the homozygous line harboring the His-to-Tyr substitution (*znf408*$^{rmc105/rmc105}$) appeared to have somewhat larger outer segments. Staining for GNAT2, a cone-specific protein, showed that in all lines, cone photoreceptor cells appeared to have properly developed, although the intensity of the GNAT2 staining was not equal in all conditions (Fig. 3c). Finally, thickness of the outer and inner nuclear layer were measured at 5, 90, and 180 dpf. Overall, no consistent differences were observed between wild-type and mutant lines, with individual differences present at some time points (Supplemental Fig. S4).

Next, to analyze the retinal vascular development, function and pathology in larval and adult mutant fish or controls, we injected fish at 5, 90, or 180 dpf with fluorescently labeled 70 kDa Dextran, a method commonly used to analyze vascular perfusion, permeability, and leakage, and investigated the retinal vasculature by confocal microscopy. At 5 dpf, we found a significantly reduced number of hyaloid vessels formed in all three homozygous mutant strains, as well as in heterozygous missense (*znf408*$^{rmc105/+}$) mutants (Fig. 4), leading to significantly reduced hyaloid vascular density (Supplemental Fig. S5). Ongoing hyaloid angiogenesis at these developmental stages was apparent by the presence of several vascular sprouts in all groups, but there were no significant differences in sprouting across the genotypes analyzed (Supplemental Fig. S6). The hyaloid vessels that did develop, however, were well perfused and did not leak fluorescently labeled dextran from the plasma into the tissue (Fig. 4a and Supplemental Figure S6). In contrast to this early phenotype, homozygous mutant fish at 90 dpf developed robust retinal neovascularization as evidenced by widespread ectopic sprouting of retinal capillaries (Figs. 4a and c and Supplemental Figure S6). These new sprouts were thin and nonfunctional and as such did not support perfusion (Fig. 4a) and did not significantly increase the density of the retinal vasculature, except for the *znf408*$^{rmc103/rmc103}$ strain (Supplemental Fig. S5). Importantly, the vessels were also not leaky at this time point, as no fluorescently labeled dextran was found outside the vascular lumen (Fig. 3a and Supplemental Fig. S6). Interestingly, at later stages of disease development represented by 180 dpf fish, the unstable and nonperfused sprouts seen in the 90 dpf fish had largely regressed (Fig. 4a), although a smaller yet statistically significant number of ectopic sprouts still remained (Supplemental Fig. S6). The retinal vascular density had, however, returned to wild-type levels in the *znf408*$^{rmc103/rmc103}$ strain (Supplemental Fig. S5). Interestingly, at this stage, the retinal vasculature had become extremely leaky, as demonstrated by multiple, large edematous pools of fluorescently labeled dextran that had accumulated under the inner limiting membrane of the retina, especially in the *znf408*$^{rmc103/rmc103}$ and *znf408*$^{rmc104/rmc104}$ strains (Figs. 4a and d and Supplemental Fig. S6). Collectively, these findings demonstrate a progressive retinal vascular pathology developing in *znf408*-mutant zebrafish characterized by initially impaired hyaloid vessel development, followed by exaggerated retinal sprouting and that culminates in robust leakage and retinal edema. Importantly, this trajectory closely recapitulates the vascular changes found in patients with FEVR.

To assess if there is any visual impairment in these zebrafish, 5 dpf zebrafish larvae were subjected to visual motor response assay. In this assay, 24 wild-type and 24 mutant larvae were placed individually in a 48-well plate and were exposed to light and dark condition every 10 minutes for 4 hours. The movements of the larvae were monitored during the assay, which is measured as distance moved (in mm) and velocity (in mm/s). We focused our analysis on the startle response of the larvae to drastic light onset, such as the movement occurring during the switch from dark to light. Although significant differences in startle response between wild type and mutant larvae was not observed, there was a trend that the truncated mutant larvae, partic-
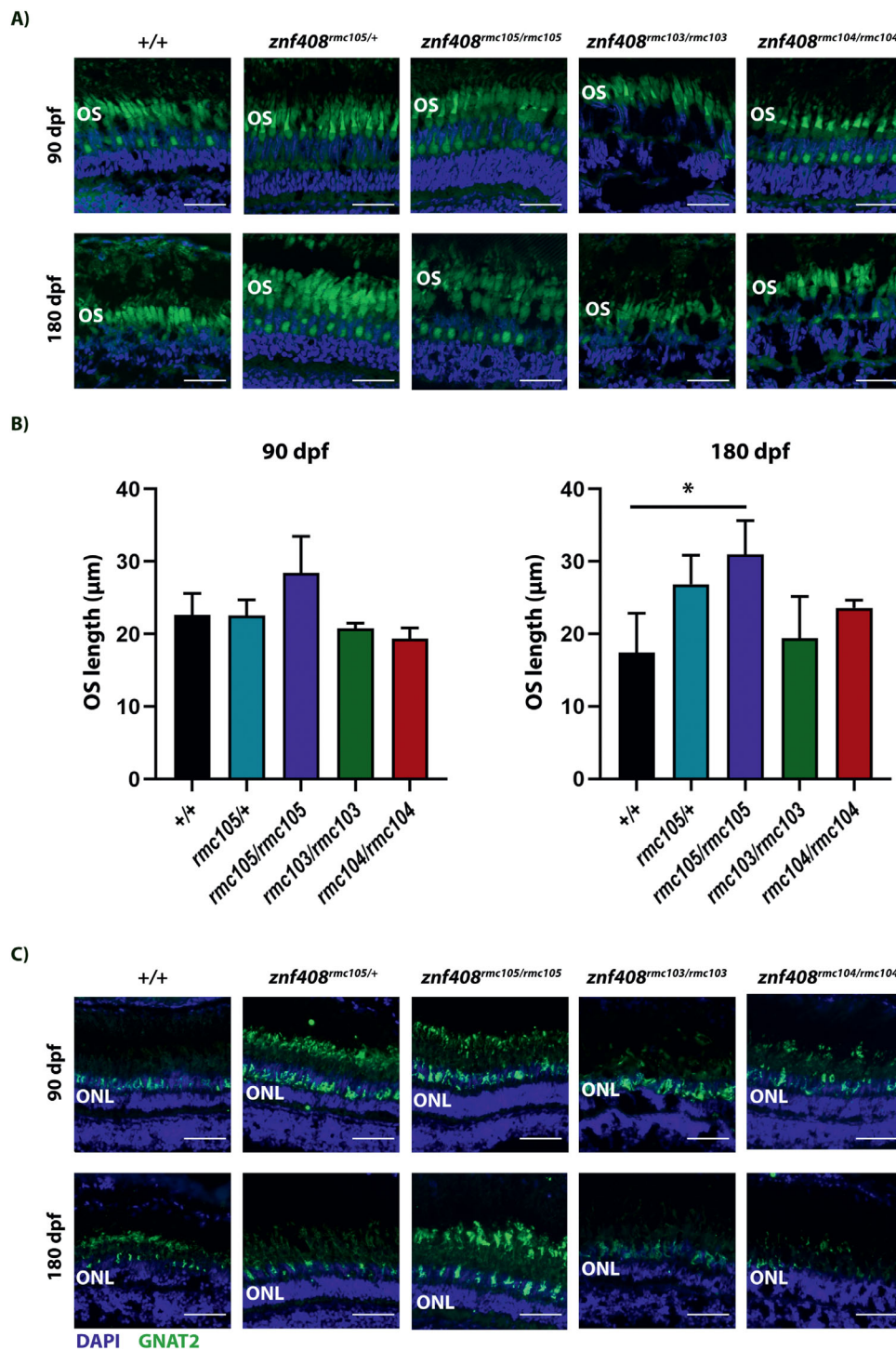
FIGURE 3. Photoreceptor characterization in adult wild-type and *znf408*-mutant zebrafish. (**a**) A representative image of Bodipy staining per condition is shown. Scale bar is 25 μm. (**b**) Quantification of OS length. At least 3 sections were analyzed per condition. *$P < 0.05$. (**c**) A representative image of Gnat2 staining per condition is shown. Scale bar is 25 μm.

ularly *znf408^rmc103/rmc103* and *znf408^rmc105/rmc105* mutants did not respond to the light switch as much as the wild-type larvae (Fig. 5). The heterozygous missense mutant (*znf408^rmc105/+*) unexpectedly showed more response to light switch compared with wild-type zebrafish, albeit insignificant.

DISCUSSION

The identification of a mutation in *ZNF408* in an autosomal dominant FEVR family followed by further in vitro investigation has indicated its role in the development of vasculature.[4,23] To further study *ZNF408* in vivo, we generated two truncated (*znf408^rmc103/rmc103* and *znf408^rmc104/rmc104*) and
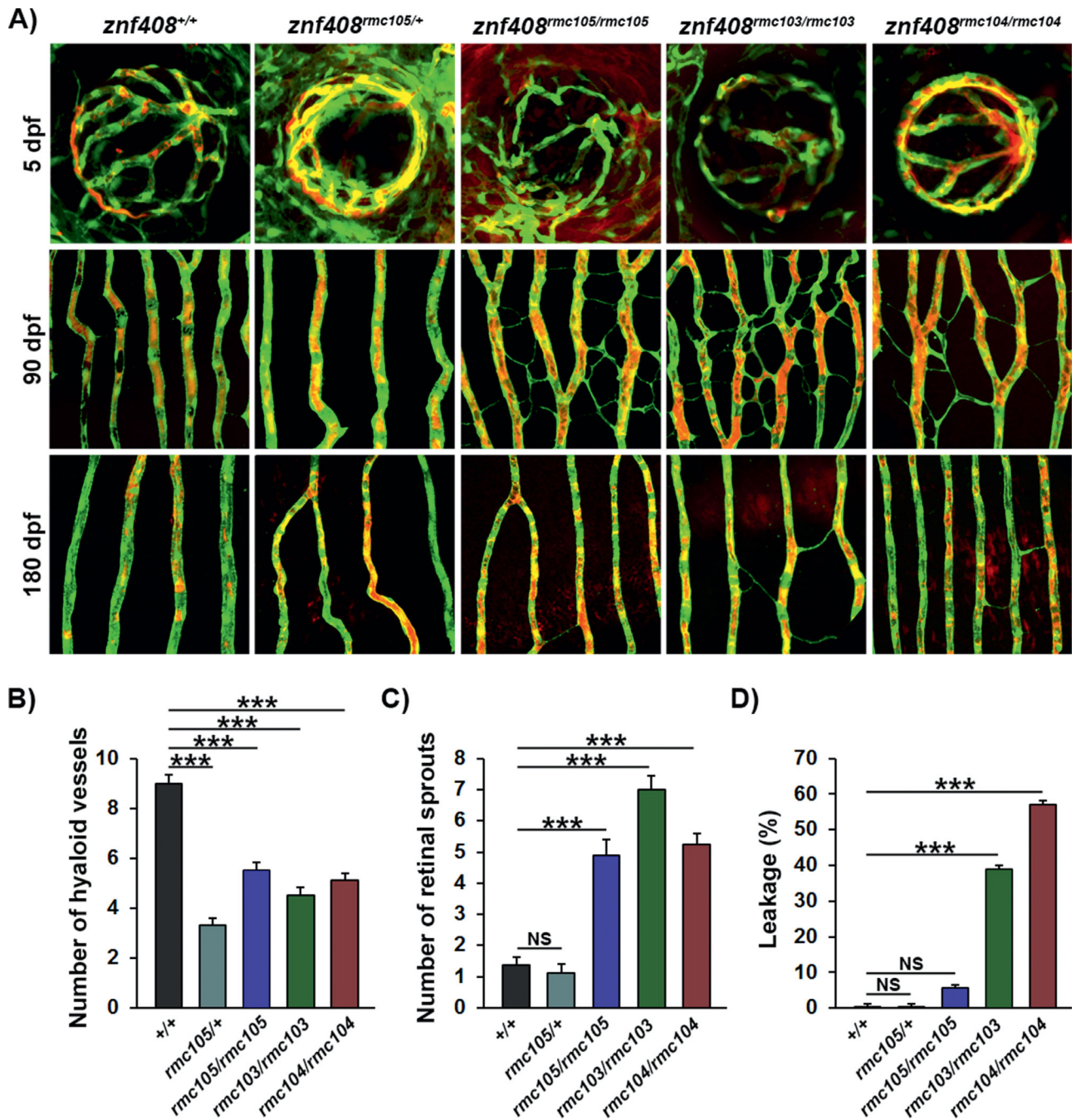
FIGURE 4. Progressive vascular pathology in *znf408*-mutant zebrafish larvae and adults. (**a**) Confocal micrographs at 5, 90, or 180 days postfertilization (dpf) of the hyaloid (5 dpf, top row) or retinal vessels (90 dpf, second row and 180 dpf, third row) in *znf408*^{+/+}, *znf408*[rmc105/+], *znf408*[rmc105/rmc105], *znf408*[rmc103/rmc103], and *znf408*[rmc104/rmc104] zebrafish crossed onto the *Tg(flk1:GFP)* background (vessels shown in green) following injection with rhodamine-conjugated dextran (plasma shown in red). (**b**) Quantification of the number of hyaloid vessels at 5 dpf from the groups shown in (**a**). n = 10, ANOVA: $P < 0.001$, Dunnett's post hoc: ***$P < 0.001$. (**c**) Quantification of the number of sprouts in the retinal vessels at 90 dpf from the groups shown in (**a**). n = 10, ANOVA: $P < 0.001$, Dunnett's post hoc: ***$P < 0.001$. (**d**) Quantification of the leaked dextran as a percentage of total dextran in the retinal vasculature at 180 dpf from the groups shown in (**a**). n = 10, ANOVA: $P < 0.001$, Dunnett's post hoc: ***$P < 0.001$.

one missense (*znf408*[rmc105/rmc105]) zebrafish model using CRISPR/Cas9 technology. Mutant transcripts were generated and did not seem to fully undergo nonsense-mediated decay; in fact, the expression of *znf408* appeared to be somewhat higher in mutant lines compared with wild-type zebrafish. Immunohistochemistry analysis failed to reliably detect znf408 in zebrafish retina, possibly because of the poor conservation between the human and zebrafish amino acid sequence of ZNF408 in the region of the epitope. Nevertheless, the zebrafish models we generated clearly showed retinal vascular phenotypes at 5 dpf, 90 dpf, and 180 dpf.
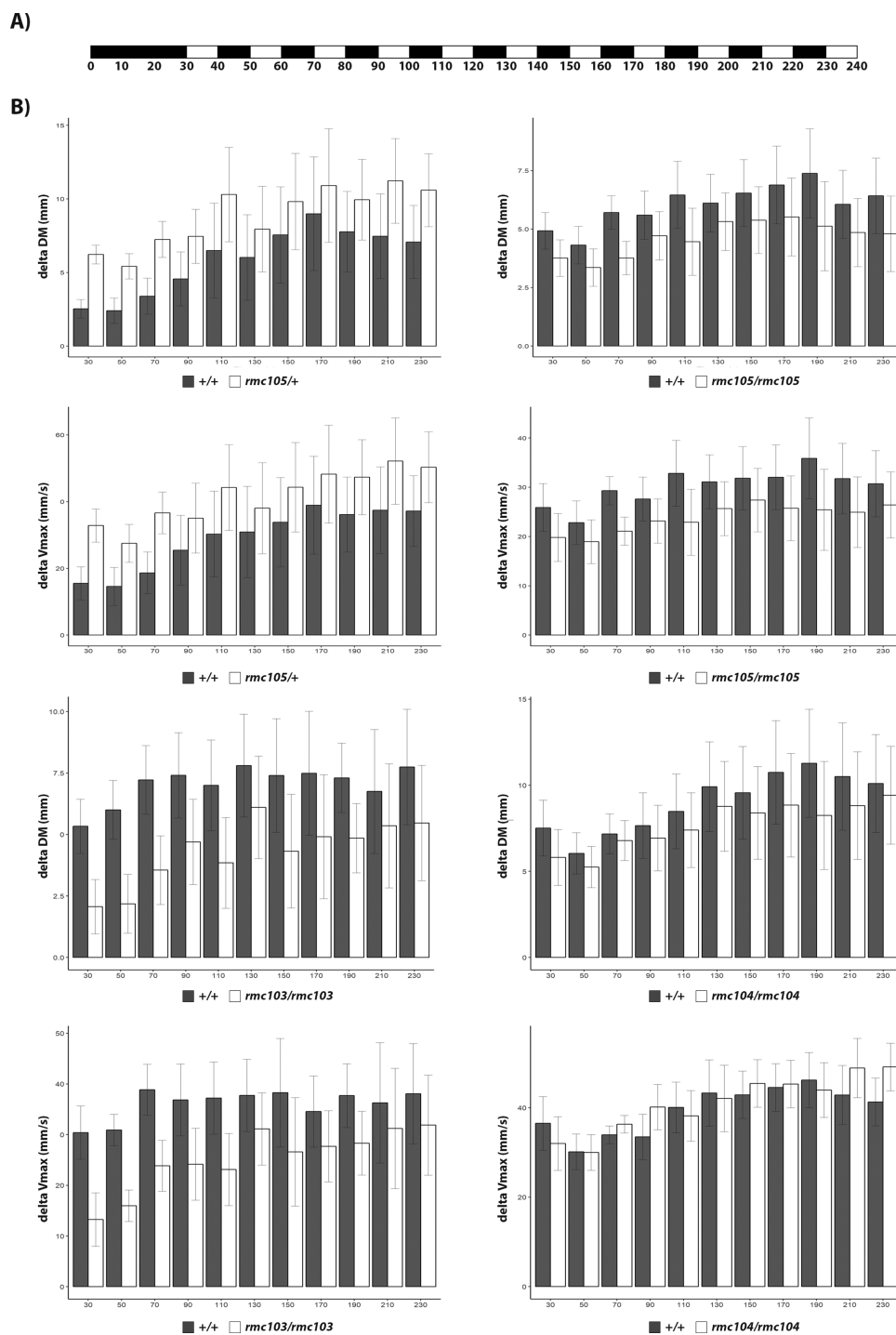
FIGURE 5. Homozygous mutant larvae appear to have less visuomotor response towards light. (**a**) A schematic overview of the light treatment given to the 5 dpf larvae. Black bars denotes dark (lights OFF), whereas white bars illustrates light (lights ON) condition. Numbers underneath the bars indicate the duration of the condition in minutes. (**b**) Bar graphs showing the startle response of wild-type versus mutant larvae. Startle response is stated as delta distance moved (DM, in mm) or delta maximum velocity (Vmax, in mm/s). Delta DM or delta Vmax was defined as average DM or Vmax at light ON+1 second and light ON+2 seconds subtracted by the average DM or Vmax 30 seconds before lights ON.

The presence of a zebrafish ortholog for the majority of known human disease genes and its genetic versatility render it a suitable animal model to study gene function. Moreover, the similarity of its retinal structure to that of humans, and the availability of vasculature-specific transgenic reporter lines, allowed observation of retinal vasculature development in a disease context, such as intended in this study. Although phenotypic discrepancy between morpholino and gene editing studies in zebrafish has been reported,[15–17] this was not the case for *znf408*. At the larval stage, *znf408* mutant zebrafish showed delayed retinal vasculature development, similar to that observed

previously in morpholino-mediated knockdown experiments.[4] This suggests the specificity of the phenotype observed upon *znf408* modification with either method. The use of gene editing to generate stable *znf408* zebrafish mutants allowed us to follow-up the phenotypic observations to adult stages.

All three mutant lines exhibited similar pathological hyaloid or retinal vascular features, strongly indicating that these phenotypes were caused by specific modification of *znf408* function in these strains. In all three strains, hyaloid vessel development was stunted, suggesting that *znf408* is important for angiogenesis specifically in the hyaloid vasculature. In juvenile (3 months old) mutants, however, ectopic capillary sprouting in the peripheral retina was evident, a phenotype highly reminiscent of hypoxia-induced capillary sprouting,[21,22] suggesting that the initially underdeveloped retinal vasculature likely led to retinal hypoxia, which in turn drove ectopic capillary sprouting. At 6 months, the immature capillary sprouts had regressed but the capillary network remained immature and highly leaky. These phenotypes closely resemble the vascular pathologies seen during progression of FEVR in humans, which also begin with a retinal vasculopathy but at more advanced stages progress to pathological retinal neovascularization and leakage.[2,24] As such, the functions of *znf408* in regulating the zebrafish retinal vasculature closely recapitulate that seen in humans.

ZNF408 encodes for a protein that belongs to the PRDM (positive regulatory domain I-binding factor 1/PRDI-BF1 and retinoblastoma-interacting zinc finger protein 1/RIZ1 homology domain containing) family. Such a protein typically contains a PRDM domain, which is often found in a subfamily of SET methyltransferases, and multiple adjacent C2H2 zinc finger domains. Members of this family have been reported to regulate gene expression either by enzymatic activity towards histone modification, or by interacting with other proteins to modify gene expression.[25,26] The C2H2 domains of ZNF408 are conserved in several species (i.e., *Homo sapiens*, *Bos taurus*, *Canis familiaris*, *Mus musculus,* and *Danio rerio*), highlighting their importance. *Znf408* mRNA was detectable in both truncated lines (*znf408^rmc103/rmc103* and *znf408^rmc104/rmc104*), suggesting that the mutant mRNA did not undergo nonsense-mediated decay, at least not to a large extent. Therefore, a truncated znf408 may be produced in *znf408^rmc103/rmc103* and *znf408^rmc104/rmc104* zebrafish. However, the protein is likely not functioning properly because of the disrupted zinc finger domains, hence the retinal vasculature phenotype. We have seen in *znf408^rmc105/+* fish how even a single amino acid change in the fourth C2H2 domain led to the observed phenotype, comparable to that observed in all homozygous mutant lines. However, while all mutant lines exhibited similar overall phenotypes, subtle differences in severity were apparent at the 5, 90, and 180 dpf timepoints. Whereas heterozygous *znf408^rmc105/+* mutants exhibited impaired hyaloid vessel development that was noninferior to that seen in the homozygous mutants, the heterozygous fish at 90 and 180 dpf were not phenotypically different from wild-type controls. This suggests that while the development of hyaloid vasculature was temporarily delayed in the heterozygous *znf408^rmc105/+* mutants, it likely recovered faster or more fully leading to retinal normoxia at 90 dpf compared with the homozygous mutants. Also at 180 dpf, the homozygous missense *znf408^rmc105/rmc105* mutants did not exhibit the same level of vascular leakage as in the *znf408^rmc103/rmc103* and *znf408^rmc104/rmc104* mutants that are predicted to produce truncated znf408 proteins. This suggests that in zebrafish *znf408* additional vascular functions are associated with the region downstream of the fourth zinc finger domain.

FEVR patients carry the p.His455Tyr mutation in a heterozygous manner.[4] In zebrafish, we observed a clear phenotypic difference between *znf408^rmc105/+* and *znf408^rmc105/rmc105*. Such a difference was also noted in the animal models for other FEVR genes, such as *FZD4*, *LRP5*, and *TSPAN12*, in which the heterozygous knock-out mice did not show (prominent) phenotype, although both heterozygous and homozygous mutations in these genes have been reported in FEVR patients.[2,27–29] It is still poorly understood what underlies this difference. Intriguingly, the vascular disruption observed in *znf408* mutants seemed to be specific to the hyaloid/retinal vasculature. This is in line with other studies demonstrating specific requirements for PI3K,[30] VEGF-B,[31] or vitamin D[32] in the development of the hyaloid vessels in zebrafish. The specific role of these signaling pathways and whether they constitute different points in the same pathway or contribute to several independent pathways that converge on regulating retinal vascular development is an area of future investigation.

The p.His455Tyr mutation is located within one of the C2H2 domains of ZNF408 and a previous study has shown that endothelial cells overexpressing p.His455Tyr ZNF408 failed to form tube networks *in vitro*. Subsequent transcriptome analysis revealed that ZNF408 regulates the expression of genes involved in the development of vasculature, a process that appears to be disrupted by the p.His455Tyr mutation.[23] Taking into account the comparable *in vitro* versus *in vivo* phenotype, it is tempting to hypothesize that *znf408* has a similar molecular role in zebrafish and the phenotype observed is due to gene expression perturbances. Further investigation to the transcriptome of the mutant zebrafish models may shed further light on this. Analysis performed at different time points may also deepen our insight into the molecular dynamics leading to the unique phenotypes observed at the different stages.

We attempted to detect znf408 protein in the zebrafish retina by immunohistochemistry. Znf408 appeared to localize to the outer plexiform layer in the wild-type zebrafish larvae. However, a similar signal was also detected in *znf408^rmc103/rmc103* and *znf408^rmc104/rmc104*, although the antibody epitope should not be present in case a truncated znf408 is expressed in the mutant models. Furthermore, no reliable signal was obtained in the retina of young adult (3 mpf) and adult (6 mpf) zebrafish. Materials only stained with the secondary antibody did not give any fluorescent signal, indicating that there is no aspecific binding of the secondary antibody. In addition, the fluorescent signal was only obtained if the zebrafish materials were not fixed before cryosectioning. It is possible that there is not enough similarity between the epitope of the primary znf408 antibody used and the zebrafish znf408 amino acid sequence. The specificity of the antibody was previously tested by immunocytochemistry on a cellular system overexpressing HA-tagged znf408, and the fluorescent signal of the HA-tag and znf408 were overlapping, suggesting that the antibody used, in theory, could recognize zebrafish znf408, albeit overexpressed. Nevertheless, we cannot exclude whether there is any peptide in zebrafish that resembles the epitope of the primary antibody, hence the signal observed in *znf408^rmc103/rmc103* and *znf408^rmc104/rmc104* mutant lines. A primary antibody directed specifically against zebrafish znf408, in combination with blocking peptides, will likely

yield more reliable results. A detailed characterization of photoreceptor outer segment length, cone photoreceptor staining, and thickness of the outer and inner nuclear layers revealed some individual variation between wild-type fish and one of the mutant lines in one or more of these aspects. However, as none of the changes we observed were consistent for one or the other mutant; these differences can most likely be attributed to variations between individual fish lines as well as between experiments.

This study corroborates the involvement of *ZNF408* in the development of retinal vasculature and also in the disease mechanism of FEVR. Intriguingly, in humans, biallelic loss-of-function mutations in *ZNF408* have been reported to underlie autosomal recessive retinitis pigmentosa.[33,34] The loss of function znf408 zebrafish models (as in *znf408*[rmc103/rmc103] and *znf408*[rmc104/rmc104]) showed defective retinal vasculature development and only mild visual impairment in visuomotor assay, particularly if compared with the visual impairment observed in retinitis pigmentosa zebrafish models.[35–37] One explanation for this is that the visuomotor assay we used here is not sensitive enough, and alternatives (e.g., electroretinogram recordings, optokinetic response measurements) would be needed. Thus, it is yet to be determined how (predicted) loss of function of *znf408* (as in *znf408*[rmc103/rmc103] and *znf408*[rmc104/rmc104]) showed a retinal vasculature phenotype instead of retinitis pigmentosa-like symptoms in zebrafish. If truncated znf408 is present in *znf408*[rmc103/rmc103] and *znf408*[rmc104/rmc104], it is well possible that the absence of the C-terminal part of znf408 (including 6 of 10 predicted C2H2 domains) did not, or at least not entirely, disrupt photoreceptor function, despite the apparent vasculature damage. That protein-truncating mutations affecting the N-terminal part of the human ZNF408 protein, as well as a missense mutation in one of the C2H2 domains (p.Arg541Cys) underlie recessive RP and thus do affect photoreceptor function can be explained by interspecies differences (zebrafish vs. humans), the presence or absence of truncated proteins, or by mechanisms that yet remain to be identified. Generation of a full *znf408* knock-out model, in which the indels are inserted as early as possible in *znf408* may provide further insight. Moreover, deeper molecular studies of our zebrafish models by using e.g. transcriptome analysis will likely increase our understanding on this apparent discrepancy.

In conclusion, we show here that disruption of *znf408*, as well as the introduction of a missense mutation mimicking *ZNF408*-associated FEVR, in zebrafish leads to abnormal development and function of the retinal vasculature system. To our knowledge, these are the first stable models in zebrafish generated to study *ZNF408*, which can increase our knowledge on the development of retinal vasculature in general, and the still largely unknown mechanisms on how mutations in *ZNF408* can lead to FEVR in humans.

Disclosure: **D.W. Karjosukarso**, None; **Z. Ali**, None; **T.A. Peters**, None; **J.Q. Cheng Zhang**, None; **A.D.M. Hoogendoorn**, None; **A. Garanto**, None; **E. van Wijk**, None; **L.D. Jensen**, None; **R.W.J. Collin**, None

References

1. Bek T. Regional morphology and pathophysiology of retinal vascular disease. *Prog Retin Eye Res*. 2013;36:247–259.

2. Gilmour DF. Familial exudative vitreoretinopathy and related retinopathies. *Eye (Lond)*. 2015;29:1–14.

3. Nikopoulos K, Venselaar H, Collin RW, et al. Overview of the mutation spectrum in familial exudative vitreoretinopathy and Norrie disease with identification of 21 novel variants in FZD4, LRP5, and NDP. *Hum Mutat*. 2010;31:656–666.

4. Collin RW, Nikopoulos K, Dona M, et al. ZNF408 is mutated in familial exudative vitreoretinopathy and is crucial for the development of zebrafish retinal vasculature. *Proc Natl Acad Sci U S A*. 2013;110:9856–9861.

5. Wu JH, Liu JH, Ko YC, et al. Haploinsufficiency of RCBTB1 is associated with Coats disease and familial exudative vitreoretinopathy. *Hum Mol Genet*. 2016;25:1637–1647.

6. Dixon MW, Stem MS, Schuette JL, Keegan CE, Besirli CG. CTNNB1 mutation associated with familial exudative vitreoretinopathy (FEVR) phenotype. *Ophthalmic Genet*. 2016;37:468–470.

7. Panagiotou ES, Sanjurjo Soriano C, Poulter JA, et al. Defects in the cell signaling mediator beta-catenin cause the retinal vascular condition FEVR. *Am J Hum Genet*. 2017;100:960–968.

8. Richardson R, Tracey-White D, Webster A, Moosajee M. The zebrafish eye-a paradigm for investigating human ocular genetics. *Eye (Lond)*. 2017;31:68–86.

9. Chhetri J, Jacobson G, Gueven N. Zebrafish–on the move towards ophthalmological research. *Eye (Lond)*. 2014;28:367–380.

10. Kaufman R, Weiss O, Sebbagh M, et al. Development and origins of zebrafish ocular vasculature. *BMC Dev Biol*. 2015;15:18.

11. Kitambi SS, McCulloch KJ, Peterson RT, Malicki JJ. Small molecule screen for compounds that affect vascular development in the zebrafish retina. *Mech Dev*. 2009;126:464–477.

12. Alvarez Y, Cederlund ML, Cottell DC, et al. Genetic determinants of hyaloid and retinal vasculature in zebrafish. *BMC Dev Biol*. 2007;7:114.

13. Lawson ND, Weinstein BM. In vivo imaging of embryonic vascular development using transgenic zebrafish. *Dev Biol*. 2002;248:307–318.

14. Choi J, Dong L, Ahn J, Dao D, Hammerschmidt M, Chen JN. FoxH1 negatively modulates flk1 gene expression and vascular formation in zebrafish. *Dev Biol*. 2007;304:735–744.

15. Eisen JS, Smith JC. Controlling morpholino experiments: don't stop making antisense. *Development*. 2008;135:1735–1743.

16. Schulte-Merker S, Stainier DY. Out with the old, in with the new: reassessing morpholino knockdowns in light of genome editing technology. *Development*. 2014;141:3103–3104.

17. Kok FO, Shin M, Ni CW, et al. Reverse genetic screening reveals poor correlation between morpholino-induced and mutant phenotypes in zebrafish. *Dev Cell*. 2015;32:97–108.

18. Gagnon JA, Valen E, Thyme SB, et al. Efficient mutagenesis by Cas9 protein-mediated oligonucleotide insertion and large-scale assessment of single-guide RNAs. *PLoS One*. 2014;9:e98186.

19. Bladen CL, Navarre S, Dynan WS, Kozlowski DJ. Expression of the Ku70 subunit (XRCC6) and protection from low dose ionizing radiation during zebrafish embryogenesis. *Neurosci Lett*. 2007;422:97–102.

20. Slijkerman R, Goloborodko A, Broekman S, et al. Poor Splice-Site Recognition in a Humanized Zebrafish Knockin Model for the Recurrent Deep-Intronic c.7595-2144A>G Mutation in USH2A. *Zebrafish*. 2018;15:597–609.

21. Cao R, Jensen LD, Soll I, Hauptmann G, Cao Y. Hypoxia-induced retinal angiogenesis in zebrafish as a model to study retinopathy. *PLoS One*. 2008;3:e2748.

22. Rouhi P, Jensen LD, Cao Z, et al. Hypoxia-induced metastasis model in embryonic zebrafish. *Nat Protoc*. 2010;5:1911–1918.

23. Karjosukarso DW, van Gestel SHC, Qu J, et al. An FEVR-associated mutation in ZNF408 alters the expression of genes involved in the development of vasculature. *Hum Mol Genet*. 2018;27:3519–3527.

24. Kashani AH, Brown KT, Chang E, Drenser KA, Capone A, Trese MT. Diversity of retinal vascular anomalies in patients with familial exudative vitreoretinopathy. *Ophthalmology*. 2014;121:2220–2227.

25. Fog CK, Galli GG, Lund AH. PRDM proteins: important players in differentiation and disease. *Bioessays*. 2012;34:50–60.

26. Hohenauer T, Moore AW. The Prdm family: expanding roles in stem cells and development. *Development*. 2012;139:2267–2282.

27. Xu Q, Wang Y, Dabdoub A, et al. Vascular development in the retina and inner ear: control by Norrin and Frizzled-4, a high-affinity ligand-receptor pair. *Cell*. 2004;116:883–895.

28. Kato M, Patel MS, Levasseur R, et al. Cbfa1-independent decrease in osteoblast proliferation, osteopenia, and persistent embryonic eye vascularization in mice deficient in Lrp5, a Wnt coreceptor. *J Cell Biol*. 2002;157:303–314.

29. Junge HJ, Yang S, Burton JB, et al. TSPAN12 regulates retinal vascular development by promoting Norrin- but not Wnt-induced FZD4/beta-catenin signaling. *Cell*. 2009;139:299–311.

30. Alvarez Y, Astudillo O, Jensen L, et al. Selective inhibition of retinal angiogenesis by targeting PI3 kinase. *PLoS One*. 2009;4:e7867.

31. Jensen LD, Nakamura M, Brautigam L, et al. VEGF-B-Neuropilin-1 signaling is spatiotemporally indispensable for vascular and neuronal development in zebrafish. *Proc Natl Acad Sci U S A*. 2015;112:E5944–E5953.

32. Merrigan SL, Kennedy BN. Vitamin D receptor agonists regulate ocular developmental angiogenesis and modulate expression of dre-miR-21 and VEGF. *Br J Pharmacol*. 2017;174:2636–2651.

33. Habibi I, Chebil A, Kort F, Schorderet DF, El Matri L. Exome sequencing confirms ZNF408 mutations as a cause of familial retinitis pigmentosa. *Ophthalmic Genet*. 2017;38:494–497.

34. Avila-Fernandez A, Perez-Carro R, Corton M, et al. Whole-exome sequencing reveals ZNF408 as a new gene associated with autosomal recessive retinitis pigmentosa with vitreal alterations. *Hum Mol Genet*. 2015;24:4037–4048.

35. Corral-Serrano JC, Messchaert M, Dona M, et al. C2orf71a/pcare1 is important for photoreceptor outer segment morphogenesis and visual function in zebrafish. *Sci Rep*. 2018;8:9675.

36. Dona M, Slijkerman R, Lerner K, et al. Usherin defects lead to early-onset retinal dysfunction in zebrafish. *Exp Eye Res*. 2018;173:148–159.

37. Messchaert M, Dona M, Broekman S, et al. Eyes shut homolog is important for the maintenance of photoreceptor morphology and visual function in zebrafish. *PLoS One*. 2018;13:e0200789.